Pharmacophore Modeling and Virtual Screening Studies of Checkpoint Kinase 1 Inhibitors

Jin-Juan Chen, Ting-Lin Liu, Li-Jun Yang, Lin-Li Li, Yu-Quan Wei, and Sheng-Yong Yang*

State Key Laboratory of Biotherapy, West China Hospital, West China School of Pharmacy, Sichuan University; Sichuan 610041, China. Received January 21, 2009; accepted April 8, 2009; published online April 14, 2009

In this study, chemical feature-based 3-dimensional (3D) pharmacophore models of Checkpoint kinase 1 (Chk1) inhibitors were developed based on the known inhibitors of Chk1. The best pharmacophore model Hypo1 was characterized by the best correlation coefficient (0.9577), and the lowest root mean square deviation (0.8871). Hypo1 consists of one hydrogen-bond acceptor, one hydrogen-bond donor, and two hydrophobic features, as well as one excluded volume. This pharmacophore model was further validated by both test set and cross validation methods. A comparison analysis of Hypo1 with chemical features in the active site of Chk1 indicates that the pharmacophore model Hypo1 can correctly reflect the interactions between Chk1 and its ligands. Then Hypo1 was used to screen chemical databases, including Specs and Chinese Nature Product Database (CNPD) for potential lead compounds. The hit compounds were subsequently subjected to filtering by Lipinski's rule of five and docking study to refine the retrieved hits. Finally some of the most potent (estimated) compounds were selected from the final refined hits and suggested for further experimental investigation.

Key words Checkpoint kinase 1; kinase inhibitor; pharmacophore model; virtual screening

Checkpoint kinase 1 (Chk1), a serine/threonine kinase, plays a critical role in the regulation of the cell-cycle G2/M checkpoint.[1—3] When DNA damage is detected in human cells, as a response, Chk1 is activated through ATM/ATR pathway. The activated Chk1 triggers the G2/M checkpoint, which arrests the cells in G2 to allow time for repairing their DNA. The inhibition of Chk1 kinase has been shown to result in abrogation of the G2/M checkpoint, which would permit premature mitotic entry in the presence of DNA damage, leading ultimately to cell death.[4—6] This suggests a potential therapeutic use of Chk1 inhibitors in cancer therapy; that is as sensitizing agents of DNA damaging drugs which are still a major component of cancer therapy.[3,7—9] Indeed, several Chk1 inhibitors, including UCN-01[10] and SB-218078,[2,11] have been reported to be able to enhance the cytotoxicities of the standard DNA-damaging agents *in vivo*. In addition, selective Chk1 inhibitors are also helpful in the study of G2/M checkpoint signaling.[3,12] Therefore, development of Chk1 inhibitors has attracted much attention in recent years.

Currently, many academic institutes and pharmaceutical companies have been involved in the development of Chk1 inhibitors. And a considerable number of compounds have been reported to have inhibitory potency against Chk1. Some compounds, such as PF-477736, AZD7762 and UCN-01,[9,12,13] have entered into clinical trials. Even so, discovering more potent Chk1 inhibitors with novel chemical structures are still needed and important in order to provide more lead candidates for the drug development.

Quantitative structure–activity relationship (QSAR) methods, particularly three dimensional QSAR (3D-QSAR), have been demonstrated as an effective tool in discovering novel lead compounds.[14,15] And pharmacophore modeling method is one of the best 3D-QSAR methods, which has been successfully applied to the drug discovery.[16—20] Thus, in this investigation, we shall first develop 3D pharmacophore models of Chk1 inhibitors based on the known Chk1 inhibitors. It is expected that the established pharmacophore models are able to correctly elucidate the QSAR of the Chk1 inhibitors. Then the best pharmacophore model obtained will be used to screen chemical libraries to identify new inhibitors against Chk1.

Experimental

Pharmacophore Modeling All the pharmacophore modeling calculations were carried out by using CATALYST 4.11 software package (Accelrys, San Diego, U.S.A.).[21] The common pharmacophore features necessary for potent Chk1 inhibitors were identified by HipHop program, and quantitative pharmacophore models were created by HypoRefine module within CATALYST.

In pharmacophore modeling, the selection of training set compounds is critical to the quality of produced models. Each modeling algorithm has its own requirements that should be conformed to, particularly in the aspects of chemical structural diversity and bioactivity variation of the training set compounds. For the pharmacophore modeling algorithm adopted here, the requirements for the training set compounds include: (1) $>=15$ compounds necessary to assure statistical power; (2) activity should span at least 4 orders of magnitude; (3) each order of magnitude represented by $>=3$ compounds; (4) compounds with similar structures should differ in activity by at least one order of magnitude; and (5) compounds with similar activity must be structurally distinct. According to these criteria, we carefully chose twenty-two Chk1 inhibitors, which were collected from different literature resources,[22—32] to form a training set for the generation of quantitative pharmacophore models. Their IC_{50} (half maximal inhibitory concentration) values span a range of 6 orders of magnitude (from 0.5 to 31800 nM). And the other three criteria mentioned above are also satisfied. Structures and biological activities of these compounds are shown in Chart 1 (**1**—**22**). The five most active compounds (**1**—**5**) in the training set were selected for the identification of common chemical features by HipHop.

All molecules were built in CATALYST 2D/3D visualizer in CATALYST software package and were minimized to the closest local minimum using the Charmm-like force field[33] implemented in the program. A series of energetically reasonable conformational models which represent the flexibility of each compound were generated within the CATALYST CatConf module using the Poling Algorithm.[34] We set the maximum number of conformers to 250, and the energy threshold above the global energy minimum to 20 kcal/mol. Default settings were kept for the other parameters.

In the HipHop run, compound **1** was considered as a reference molecule, specifying a 'principal' value of 2 and a 'MaxOmitFeat' value of 0. The 'principal' and 'MaxOmitFeat' values were set to 1 for the other four most active compounds. The initial features, which were specified based on an overview of all the training set molecules, included hydrogen-bond acceptor (A), hydrogen-bond donor (D), hydrophobic (H), ring aromatic (R), Hydrophobic aromatic (Y) and hydrophobic aliphatic (Z) features. In the Hy-

* To whom correspondence should be addressed. e-mail: yangsy@scu.edu.cn

© 2009 Pharmaceutical Society of Japan

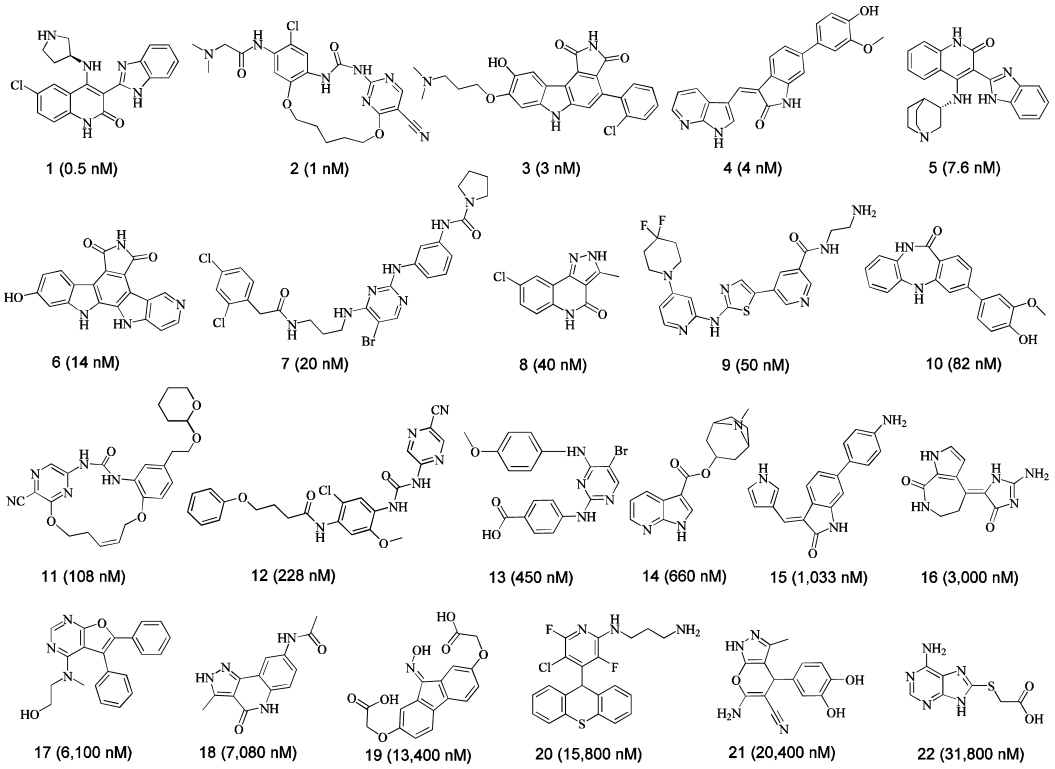

Chart 1. Chemical Structures of the 22 Training Set Compounds Together with Their Experimental Activity Data (IC_{50} Values, nM)

poRefine run, the initial pharmacophore features were specified based on the common pharmacophore features identified in the HipHop run. The 'Spacing' value was assigned to 120. The "Uncertainty" value was set to 3. And default settings for other parameters were employed.

Assessment of Pharmacophore Models Test set and cross validation methods were used for assessing the performance of the generated pharmacophore models. For the use of test set method, 232 compounds with different bioactivities and structures were selected to form a test set (see Table S1 in Supplementary Material). All of the test set compounds were prepared using the same method as that for the training set. The performance of pharmacophore model was examined by utilizing the pharmacophore model to regress against the test set compounds. The cross validation was carried out by using CatScramble[35] program within CATALYST. This procedure tries to scramble the experimental activities in the training set randomly, and the resulting training sets are used for HypoRefine runs. The confidence level was set to 95%. Thereby CatScramble program generated 19 random spreadsheets to construct hypotheses using exactly the same conditions as used in generating the original pharmacophore hypotheses.

Database Screening The best HypoRefine pharmacophore hypothesis was used as a 3D structural search query for retrieving potent molecules from chemical databases including Specs and Chinese Nature Product Database (CNPD). All queries were performed using the "Best Flexible Search Databases/Spreadsheets" method within the CATALYST DBServer module. Only those compounds that fit all the features of the pharmacophore model in the CATALYST queries were retrieved as a hit.

Docking Study The docking study was carried out by LigandFit program within Cerius2 program package (Accelrys, San Diego, U.S.A.),[36] and the Dreiding force field was used for all calculations. The crystal structure of Chk1 complexed with CHIR-124[28] (PDB entry: 2GDO), taken from Protein Data Bank,[37] was used as reference protein. Solvent molecules in the crystal structure were removed. Hydrogen atoms were added in a normal scheme by Cerius2. The binding site of the bound ligand was identified as the active site. The site definition as well as the used docking parameters was firstly validated through docking the bound ligand back into the protein. The best docked pose should differ only minimally from the position of the ligand in the crystal structure (for example, root mean square deviation (rmsd) is <1.0 Å). Partial charges of all chemical compounds were automatically assigned by the Gasteiger scheme implemented in Cerius2 program. Conformations of each compound were created with Monte Carlo simulation (5000 trials) and flexible fit was selected. Within LigandFit, several scoring functions including LigScore1, LigScore2,[38] PLP1, PLP2,[39] Jain,[40] Ludi1, Ludi2, Ludi3,[41,42] PMF,[43] as well as a consensus score,[44] are available. Since there is no generally applicable scoring function so far, a solution to this problem is the calculation of a consensus score, which makes use of the merits of different scoring functions by combining their results. We first defined a consensus score by nine scoring functions, including LigScore1, LigScore2, PLP1, PLP2, Jain, Ludi1, Ludi2, Ludi3 and PMF. The consensus score was then validated by a set of selected compounds, which IC_{50} values span a range of 6 orders of magnitude (compounds **1**, **3**, **5**, **10**, **11**, **13**, **14**, **16**, **18**, **21**, see Chart 1). The correlation coefficient between consensus scores and experimental IC_{50} values was 0.8667, indicating that the consensus score has a good performance. Thus the consensus score will be used to sort the hit compounds in this study.

Results and Discussion

Pharmacophore Models Qualitative HipHop models were first generated based on the five most-active compounds in the training set (compounds **1**—**5**, Chart 1). The best HipHop model, shown in Fig. 1, involves four types of features, namely, hydrogen bond acceptor (A), hydrogen bond donor (D), hydrophobic (H), and ring aromatic feature (R), indicating that the four types of features are necessary for potent Chk1 inhibitors. Accordingly, in the quantitative HypoRefine modeling, the four types of features were selected as the initial input.

The quantitative models were generated with the twenty-two compounds in the training set (compounds **1**—**22**, Chart 1). The top 10 hypotheses generated by HypoRefine algorithm together with their statistical parameters are given in Table 1. The best hypothesis, corresponding to Hypo1 (Fig. 2a), contains four features, including one hydrogen-bond acceptor (A), one hydrogen-bond donor (D), and two hydrophobic features (H1 and H2). One excluded volume (E) is also involved in Hypo1. Here one may notice that the second best hypothesis Hypo2 contains the same features and ex-

cluded volume as Hypo1. The main difference between them is the spatial locations of the features and excluded volume. The 3D space and distance constraints of the pharmacophore features of Hypo1 are shown in Fig. 2b. Figures 2c and d show the alignment of Hypo1 with the most active compound **1** (IC_{50}=0.5 nM) and the least active compound **22** (IC_{50}=31800 nM) in the training set, respectively. For compound **1**, the hydrogen-bond acceptor was mapped to the second position oxygen of quinolin-2(1*H*)-one; the hydrogen-bond donor was mapped to the secondary position nitrogen of quinolin-2(1*H*)-one; the two hydrophobic features were mapped to the chlorine and the benzene ring of benzimidazole, respectively. By the way, for further understanding of Hypo1, Fig. 2e presents the alignments of the five most-active compounds (compounds **1**—**5**) with Hypo1, which clearly shows that Hypo1 was also mapped very well with the other most active compounds in the training set except compound **1**. For compound **22**, the hydrogen-bond acceptor was mapped to the oxygen atom of carbonyl group, and the hydrogen-bond donor was mapped to the ninth position nitrogen of purin. The rest two features of Hypo1 could not be matched with any moiety of this compound. All of these reflect the validity of the pharmacophore model Hypo1 to some extent.

Furthermore, we classified all the training set compounds into three categories: highly active ($IC_{50}\leq$50 nM, +++), moderately active (50 nM$<IC_{50}\leq$1000 nM, ++), and low active ($IC_{50}>$1000 nM, +). Table 2 shows the predicted and experimental inhibitory activities of these 22 molecules in the training set. Obviously most of these compounds were correctly predicted, except two compounds: one highly active compound was predicted to be moderately active, and one low active compound was predicted as moderately active one.

Validation of the Pharmacophore Model A good pharmacophore model is not only able to predict the activities of the training set compounds accurately, but also can predict the activities of external compounds of training set. Here an independent validation set containing 232 compounds whose inhibitory activity values against Chk1 have been reported publicly was used to assess the predictive ability of Hypo1. The assessment was carried out by using Hypo1 to regress against the test set compounds. Figure 3 presents the plot of

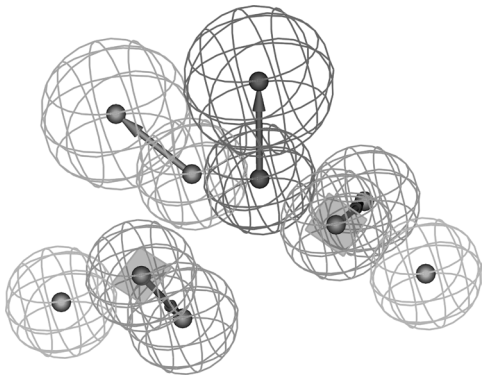

Fig. 1. The Best HipHop Model Generated by the Five Most Active Compounds (**1**—**5**) in the Training Set.

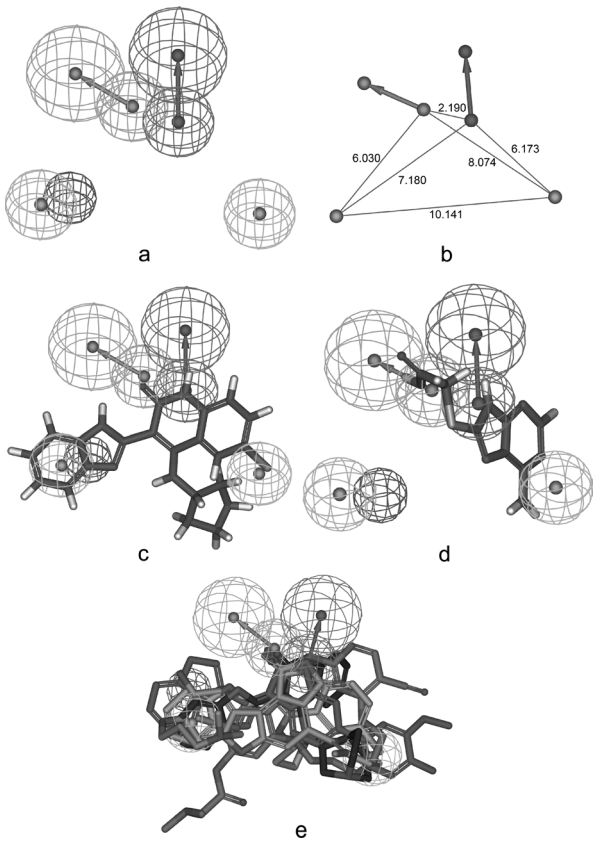

Fig. 2. Pharmacophore Models of Chk1 Inhibitors

(a) The best HypoRefine model, Hypo1; (b) 3D spatial relationship and geometric parameters of Hypo1; (c) Hypo1 mapped to the most active compound (**1**, IC_{50}=0.5 nM); (d) Hypo1 mapped to the least active compound (**22**, IC_{50}=31800 nM). (e) The alignment of the most active compounds (**1**—**5**) in training set with Hypo1.

Table 1. Statistical Parameters of the Top 10 Hypotheses of Chk1 Inhibitors Generated by HypoRefine Program

Hypo. No.	Total cost	Cost difference[a)]	Error cost	Rmsd	Correlation coefficient	Features[b)]
1	100.678	75.25	82.6555	0.8871	0.9577	ADHHE
2	102.316	73.612	84.6691	0.9849	0.9471	ADHHE
3	104.411	71.517	87.1211	1.0922	0.9341	ADHRE
4	108.748	67.18	92.1485	1.2845	0.9069	ADHR
5	110.057	65.871	92.6944	1.3037	0.9044	ADHR
6	110.133	65.795	92.5258	1.2978	0.9055	ADHR
7	110.342	65.586	92.5971	1.3003	0.9053	ADHR
8	112.097	63.831	95.057	1.3836	0.8913	ADHR
9	114.58	61.348	95.6569	1.4032	0.8897	ADHR
10	114.6	61.328	97.6437	2.0152	0.8769	ADHRE

a) (Null cost−total cost), null cost=175.928, fixed cost=90.0656. For Hypo1, weight=3.0808, configuration=14.9413. All cost values are in the unit of bits. *b*) A, D, H, R and E present hydrogen bond acceptor, hydrogen bond donor, hydrophobic feature, ring aromatic feature and exclusion volume, respectively.

Table 2. Experimental and Predicted Activities (Using Hypo1) of the Training Set Compounds

Compound No.	Experimental IC_{50} (nM)	Predicted IC_{50} (nM)	Error[a]	Fit value[b]	Experimental scale[c]	Predicted scale[c]
1	0.5	1.1	+2.2	9.26	+++	+++
2	1	1.8	+1.8	9.06	+++	+++
3	3	1.1	−2.6	9.25	+++	+++
4	4	12	+3.1	8.22	+++	+++
5	7.6	6.4	−1.2	8.51	+++	+++
6	14	48	+3.4	7.64	+++	+++
7	20	25	+1.3	7.91	+++	+++
8	40	110	+2.8	7.27	+++	++
9	50	300	+6	6.83	++	++
10	82	160	+1.9	7.12	++	++
11	108	64	−1.7	7.51	++	++
12	228	150	−1.5	7.14	++	++
13	450	51	−8.8	7.61	++	++
14	660	500	−1.3	6.62	++	++
15	1033	930	−1.1	6.35	+	++
16	3000	2200	−1.3	5.97	+	+
17	6100	6300	+1	5.52	+	+
18	7080	17000	+2.4	5.08	+	+
19	13400	3800	−3.5	5.73	+	+
20	15800	9600	−1.6	5.33	+	+
21	20400	3300	−6.2	5.80	+	+
22	31800	36000	+1.1	4.75	+	+

a) A ratio between the experimental and predicted activities. A positive value indicates that the predicted IC_{50} is higher than the experimental IC_{50}, while a negative one indicates that the predicted IC_{50} is lower than the experimental IC_{50}. *b*) Fit value indicates how well the features in the hypothesis overlap the chemical features in the compound. *c*) Activity scale: +++, $IC_{50}<50$ nM (highly active); ++, 50 nM$\leq IC_{50}<$1000 nM (moderately active); +, $IC_{50}\geq$1000 nM (low active).

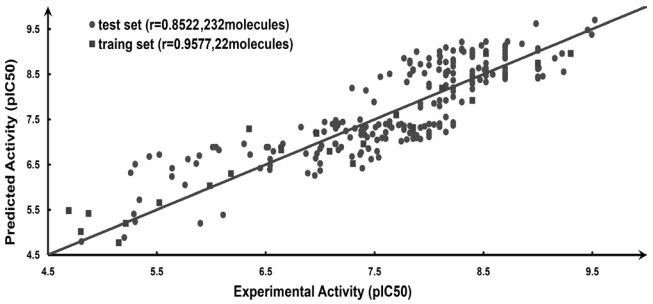

Fig. 3. Plot of the Correlation between the Experimental and Predicted Activities (by Using Hypo1) for the Test Set (Filled Circles) and the Training Set (Filled Squares) Compounds

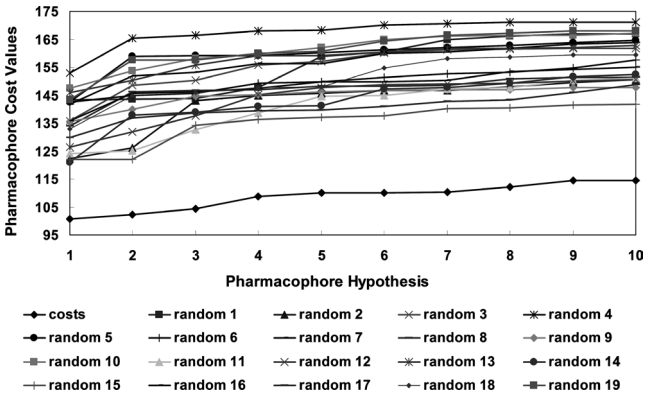

Fig. 4. The Difference in Total Cost of Hypotheses between the Initial Spreadsheet and 19 Random Spreadsheets after CatScramble Run

correlation between the experimental and predicted activities (by Hypo1) for the test set and the training set. Obviously, the correlation coefficient of 0.8522 indicates that Hypo1 is capable of predicting the IC_{50} values correctly (detailed information see Table S1 in Supplementary Material).

Further, CatScramble program within CATALYST was used to evaluate the statistical relevance of Hypo1. The purpose of this type of validation is to check whether there is a strong correlation between the chemical structures and the biological activities. In this study, a confidence level of 95% was chosen. Thus a total of 19 random spreadsheets were generated to construct hypotheses using exactly the same conditions as used in the original HypoRefine run. The total costs of pharmacophore models obtained from the 19 HypoRefine runs as well as the original HypoRefine run are presented in Fig. 4. From Fig. 4, one can see that the original hypothesis is far more superior to those of the 19 random hypotheses generated. These results provide confidence on our pharmacophore model.

A Comparison between Hypo1 and Chemical Features in the Active Site of Chk1 Protein The pharmacophore models developed here are all based on the known ligands of Chk1 protein. One may wonder whether the pharmacophore models obtained here could correctly reflect the interactions between the protein and its ligands. Very luckily, there have already been several crystal structures of Chk1-ligand complexes available in Protein Data Bank (PDB). The crystal structure of Chk1 complexed with the compound CHIR-124 (PDB entry: 2GDO) was chosen as an example since CHIR-124 is in our test set and is one of the most potent compounds ($IC_{50}=0.3$ nM).

Figure 5a presents the mapping of Hypo1 with the Chk1–CHIR-124 complex. Detailed interactions between CHIR-124 and Chk1 are depicted in Fig. 5b. From Figs. 5a and b, one can see that the hydrogen bond acceptor of Hypo1 corresponds to the hydrogen bond interaction formed between the amino acid residue Cys87 and the second position oxygen of quinolin-2(1*H*)-one. The hydrogen bond donor of Hypo1 re-

flects the hydrogen bond interaction between Glu85 and CHIR-124. The hydrophobic feature H1 of Hypo1, locating in the hydrophobic pocket formed by residues Leu15, Gly89, and Gly90, was mapped to the benzene ring. The other hydrophobic feature H2 of Hypo1, which is near to the hydrophobic pocket formed by residues Val40, Val68, Phe70, Leu82, and Leu84, was mapped to the chlorine atom of benzimidazole. The excluded volume is positioned very close to the backbone of Chk1. From here, we can conclude that the chemical features and their spatial arrangement described in the pharmacophore model Hypo1 are consistent with the actual ligand–protein interactions.

Virtual Screening The validated pharmacophore model Hypo1 was employed as a 3D search query for retrieving potent molecules from the Specs (135556) and CNPD (43055). A total of 7463 compounds were retrieved from the first screening by restricting that all the chemical features of Hypo1 must be mapped. Then these hit compounds were further subjected to filtering by applying the Lipinski's rule of five. 3889 molecules were passed through the second screening.

Docking Study All the hit compounds from the second screening were then subjected to docking study to reduce the rate of false positive. Finally, more than 20 compounds were selected from the top ranked hit compounds and suggested for further experimental assay. And ten of these compounds are given in Table S2. Figures 6a and b show a possible docking model of AK-968/12115125 (from Specs database) and the mapping of this molecule with the best pharmacophore model Hypo1.

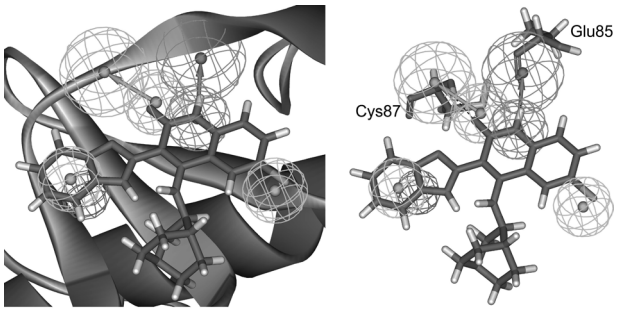

Fig. 5. (a) The Pharmacophore Model Hypo1 Positioned into the Active Site of Chk1–CHIR-214 Complex and (b) a Reduced Picture of (a) Showing the Detailed Mapping between Hypo1 and Chemical Features in the Active Site of Chk1–CHIR-214 Complex

Black dashed lines indicate hydrogen bonds.

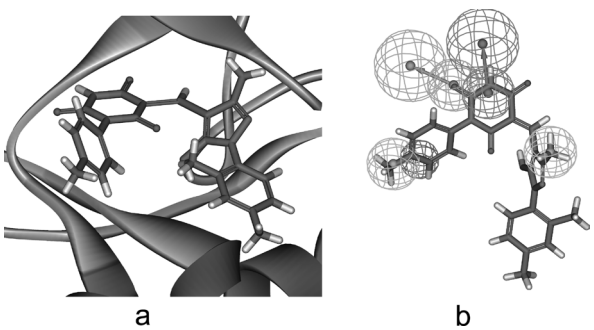

Fig. 6. (a) A Possible Docking Model of AK-968/12115125 (from Specs Database) into the Active Site of Chk1 and (b) AK-968/12115125 Aligned with the Pharmacophore Model Hypo1

Conclusions

In this study, pharmacophore modeling by using HipHop and HypoRefine modules within CATALYST program package was carried out for elucidating the structure–activity relationship of Chk1 inhibitors. The best quantitative pharmacophore model Hypo1 was characterized by the best correlation coefficient (0.9577), the lowest total cost value (100.678), the highest cost difference (75.25), and the lowest rmsd (0.8871). Hypo1 consists of one hydrogen-bond acceptor, one hydrogen-bond donor, and two hydrophobic features, as well as one excluded volume. This pharmacophore model was further validated by test set and cross validation methods. Results obtained by the test set method show a fairly good correlation between the experimental and estimated IC_{50} values, indicating a good predictive ability. And results of cross validation by using CatScramble program within CATALYST further confirmed the statistical confidence of Hypo1. A comparison analysis of Hypo1 with chemical features in the active site of Chk1 indicates that the pharmacophore model Hypo1 can correctly reflect the interactions between Chk1 and its ligands. Finally the validated model Hypo1 was used as a 3D structural query to screen two databases, namely, Specs and CNPD, for retrieving new potent inhibitors of Chk1. The hit compounds were subsequently subjected to filtering by Lipinski's rule of five and docking studies to refine the retrieved hits. Finally the most potent compounds were selected and have been suggested for further *in vitro* assays.

References

1) Luo Y., Rockow-Magnone S. K., Kroeger P. E., Frost L., Chen Z. H., Han E. K. H., Ng S. C., Simmer R. L., Giranda V. L., *Neoplasia*, **3**, 411—419 (2001).
2) Kawabe T., *Mol. Cancer Ther.*, **3**, 513—519 (2004).
3) Zhou B. B. S., Bartek J., *Nat. Rev. Cancer*, **4**, 216—225 (2004).
4) Xiao Z., Chen Z. H., Gunasekera A. H., Sowin T. J., Rosenberg S. H., Fesik S., Zhang H. Y., *J. Biol. Chem.*, **278**, 21767—21773 (2003).
5) Cuddihy A. R., O'Connell M. J., "International Review of Cytology—A Survey of Cell Biology," Academic Press Inc., San Diego, 2003.
6) Chen Y. H., Sanchez Y., *DNA Repair*, **3**, 1025—1032 (2004).
7) Zhou B. B. S., Elledge S. J., *Nature* (London), **408**, 433—439 (2000).
8) Koniaras K., Cuddihy A. R., Christopoulos H., Hogg A., O'Connell M. J., *Oncogene*, **20**, 7453—7463 (2001).
9) Janetka J. W., Ashwell S., Zabludoff S., Lyne P., *Curr. Opin. Drug Disc.*, **10**, 473—486 (2007).
10) Jiang X. X., Zhao B. G., Britton R., Lim L. Y., Leong D., Sanghera J. S., Zhou B. B. S., Piers E., Andersen R. J., Roberge M., *Mol. Cancer Ther.*, **3**, 1221—1227 (2004).
11) Chen J. S., Lin S. Y., Tso W. L., Yeh G. C., Lee W. S., Tseng H., Chen L. C., Ho Y. S., *Mol. Carcinogen*, **45**, 461—478 (2006).
12) Tse A. N., Carvajal R., Schwartz G. K., *Clin. Cancer Res.*, **13**, 1955—1960 (2007).
13) Zabludoff S. D., Deng C., Grondine M. R., Sheehy A. M., Ashwell S., Caleb B. L., Green S., Haye H. R., Horn C. L., Janetka J. W., Liu D. F., Mouchet E., Ready S., Rosenthal J. L., Queva C., Schwartz G. K., Taylor K. J., Tse A. N., Walker G. E., White A. M., *Mol. Cancer Ther.*, **7**, 2955—2966 (2008).
14) Du Q. S., Huang R. B., Chou K. C., *Curr. Protein Pept. Sci.*, **9**, 248—260 (2008).
15) Lill M. A., *Drug Discov. Today*, **12**, 1013—1017 (2007).
16) Xie H.-Z., Li L.-L., Ren J.-X., Zou J., Yang L., Wei Y.-Q., Yang S.-Y., *Bioorg. Med. Chem. Lett.*, **19**, 1944—1949 (2009).
17) Xie Q.-Q., Xie H.-Z., Ren J.-X., Li L.-L., Yang S.-Y., *J. Mol. Graph. Model.*, **27**, 751—758 (2009).
18) Wang H.-Y., Li L.-L., Cao Z.-X., Luo S.-D., Wei Y.-Q., Yang S.-Y.,

Chem. Biol. Drug Des., **73**, 115—126 (2009).
19) Wang H. Y., Cao Z. X., Li L. L., Jiang P. D., Zhao Y. L., Luo S. D., Yang L., Wei Y. Q., Yang S. Y., *Bioorg. Med. Chem. Lett.*, **18**, 4972—4977 (2008).
20) Deng X. Q., Wang H. Y., Zhao Y. L., Xiang M. L., Jiang P. D., Cao Z. X., Zheng Y. Z., Luo S. D., Yu L. T., Wei Y. Q., Yang S. Y., *Chem. Biol. Drug Des.*, **71**, 533—539 (2008).
21) ⟨http://www.accelrys.com⟩, CATALYST 4.11, Accelrys Inc., San Diego, CA.
22) Smaill J. B., Lee H. H., Palmer B. D., Thompson A. M., Squire C. J., Baker E. N., Booth R. J., Kraker A., Hook K., Denny W. A., *Bioorg. Med. Chem. Lett.*, **18**, 929—933 (2008).
23) Lefoix M., Coudert G., Routier S., Pfeiffer B., Caignard D. H., Hickman J., Pierre A., Golsteyn R. M., Leonce S., Bossard C., Merour J. Y., *Bioorg. Med. Chem.*, **16**, 5303—5321 (2008).
24) Wang L., Sullivan G. M., Hexamer L. A., Hasvold L. A., Thalji R., Przytulinska M., Tao Z. F., Li G. Q., Chen Z. H., Xiao Z., Gu W. Z., Xue J., Bui M. H., Merta P., Kovar P., Bouska J. J., Zhang H. Y., Park C., Stewart K. D., Sham H. L., Sowin T. J., Rosenberg S. H., Lin N. H., *J. Med. Chem.*, **50**, 4162—4176 (2007).
25) Tao Z. F., Wang L., Stewart K. D., Chen Z. H., Gu W., Bui M. H., Merta P., Zhang H. Y., Kovar P., Johnson E., Park C., Judge R., Rosenberg S., Sowin T., Lin N. H., *J. Med. Chem.*, **50**, 1514—1527 (2007).
26) Li G., Tao Z. F., Tong Y., Przytulinska M. K., Kovar P., Merta P., Chen Z., Zhang H., Sowin T., Rosenberg S. H., Lin N. H., *Bioorg. Med. Chem. Lett.*, **17**, 6499—6504 (2007).
27) Brnardic E. J., Garbaccio R. M., Fraley M. E., Tasber E. S., Steen J. T., Arrington K. L., Dudkin V. Y., Hartman G. D., Stirdivant S. M., Drakas B. A., Rickert K., Walsh E. S., Hamilton K., Buser C. A., Hardwick J., Tao W. K., Beek S. C., Mao X. Z., Lobell R. B., Sepp-Lorenzino L., Yan Y. W., Ikuta M., Munshi S. K., Kuo L. C., Kreatsoulas C., *Bioorg. Med. Chem. Lett.*, **17**, 5989—5994 (2007).
28) Ni Z. J., Barsanti P., Brammeier N., Diebes A., Poon D. J., Ng S., Pecchi S., Pfister K., Renhowe P. A., Ramurthy S., Wagman A. S., Bussiere D. E., Le V., Zhou Y., Jansen J. M., Ma S., Gesner T. G., *Bioorg. Med. Chem. Lett.*, **16**, 3121—3124 (2006).
29) Li G. Q., Hasvold L. A., Tao Z. F., Wang G. T., Gwaltney S. L., Patel J., Kovar P., Credo R. B., Chen Z. H., Zhang H. Y., Park C., Sham H. L., Sowin T., Rosenberg S. H., Lin N. H., *Bioorg. Med. Chem. Lett.*, **16**, 2293—2298 (2006).
30) Foloppe N., Fisher L. M., Howes R., Kierstan P., Potter A., Robertson A. G. S., Surgenor A. E., *J. Med. Chem.*, **48**, 4332—4345 (2005).
31) Lyne P. D., Kenny P. W., Cosgrove D. A., Deng C., Zabludoff S., Wendoloski J. J., Ashwell S., *J. Med. Chem.*, **47**, 1962—1968 (2004).
32) Curman D., Cinel B., Williams D. E., Rundle N., Block W. D., Goodarzi A. A., Hutchins J. R., Clarke P. R., Zhou B. B., Lees-Miller S. P., Andersen R. J., Roberge M., *J. Biol. Chem.*, **276**, 17914—17919 (2001).
33) Brooks B. R., Bruccoleri R. E., Olafson B. D., States D. J., Swaminathan S., Karplus M., *J. Comput. Chem.*, **4**, 187—217 (1983).
34) Smellie A., Teig S. L., Towbin P., *J. Comput. Chem.*, **16**, 171—187 (1995).
35) Chopra M., Gupta R., Gupta S., Saluja D., *J. Mol. Model.*, **14**, 1087—1099 (2008).
36) ⟨http://www.accelrys.com⟩, Cerius2 4.11, Accelrys Inc., San Diego, CA.
37) Berman H. M., Westbrook J., Feng Z., Gilliland G., Bhat T. N., Weissig H., Shindyalov I. N., Bourne P. E., *Nucleic Acids Res.*, **28**, 235—242 (2000).
38) Venkatachalam C. M., Jiang X., Oldfield T., Waldman M., *J. Mol. Graph. Model.*, **21**, 289—307 (2003).
39) Gehlhaar D. K., Verkhivker G. M., Rejto P. A., Sherman C. J., Fogel D. B., Fogel L., *Chem. Biol.*, **2**, 317—324 (1995).
40) Jain A., *J. Comput.-Aided Mol. Des.*, **10**, 427—440 (1996).
41) Bohm H. J., *J. Comput. Aided Mol. Des.*, **8**, 243—256 (1994).
42) Bohm H. J., *J. Comput. Aided Mol. Des.*, **12**, 309—323 (1998).
43) Muegge I., Martin Y., *J. Med. Chem.*, **42**, 791—804 (1999).
44) Clark R. D., Strizhev A., Leonard J. M., Blake J. F., Matthew J., *J. Mol. Graph. Model.*, **20**, 281—295 (2002).

Supplementary Materials

The following supplementary material is available upon request to the corresponding author.

Table S1 Chemical structures (SMILES format) of Chk1 inhibitors in the test set together with their experimentally measured and predicted (by Hypo 1) activities (IC_{50} values, nM).

Table S2 The chemical structures, fit values (bits) and predicted activities (IC_{50} values, nM) of some top ranked hit compounds from virtual screening.